Impacts of a beaver dam analogue complex on streambed vertical hydraulic gradients in a 1.2-km stream reach in Wyoming, USA

Amyel Dale L. Cero ¹, Christa A. Kelleher ², and Stephen B. Shaw ³

Corresponding Author: Amyel Dale L. Cero

Division of Environmental Science, State University of New York - College of Environmental Science and Forestry, 1 Forestry Dr, Syracuse, New York, 13210 amcero@syr.edu

Abstract

Beaver dam analogues (BDAs) have seen growing use as restoration structures across the Western US. This study investigates the patterns in streambed upwelling and downwelling along a 1.2-km stream reach in Red Canyon Creek (RCC), Wyoming before and after the installation of 31 new BDAs and the upgrade of four existing BDAs in July 2021. Over 100 mini-piezometers were used to measure upwelling and downwelling in low-flow, summer periods as quantified by vertical hydraulic gradient (VHG). Both before and after BDA installation, the stream reach was dominated by downwelling patterns, suggesting that Red Canyon Creek was a net losing stream during this summer period, with and without BDAs. While there were spatial variations in VHG before BDA installation, this variation was not dependent on stream depth, water surface concavity, sediment characteristics, and position relative to meanders, suggesting that unobservable subsurface properties may be a control on VHG or that there are attributes that were not captured due to the 10 m spacing of minipiezometers. After BDA installation, VHGs were primarily related to the magnitude of the elevation gradient across the BDA. VHGs were highest near the BDAs and diminished once more than a few meters from the BDAs. BDAs with higher elevation drops appeared to

¹ Division of Environmental Science, State University of New York - College of Environmental Science and Forestry (SUNY-ESF), Syracuse, New York

² Department of Civil and Environmental Engineering, Lafayette College, Easton, Pennsylvania

³ Department of Environmental Resources Engineering, State University of New York - College of Environmental Science and Forestry (SUNY-ESF), Syracuse, New York

induce localized hyporheic exchange near the BDA but VHGs were typically neutral more than a few meters away. When VHGs were averaged over the full reach length, BDAs appeared to slightly enhance net stream loss, albeit we could not control for possible seasonal differences in water table gradient during the observation period.

Keywords: beaver dam, beaver dam analogues, vertical hydraulic gradients, groundwatersurface water interactions

1. INTRODUCTION

In the western U.S., centuries of cattle grazing, logging, irrigation, and reduction of beaver populations have changed streams from their natural form. These changes often include channel incision, loss of pool riffle sequences, and stream bank erosion. These gross changes to channel form have secondary impacts on sediment retention, water storage, hyporheic exchange, groundwater recharge, nutrient processing, and riparian vegetation (Lautz & Fanelli, 2008; Lautz & Siegel, 2006; Pollock et al., 2014), possibly reducing ecosystem services (Wohl, 2021).

There have been multiple efforts to restore streams to their more natural form through the implementation of a variety of practices. This has included riparian zone revegetation, livestock exclusion, addition of woody debris, building of cross vanes and bank vanes, and bank stabilization. A specialized approach that incorporates aspects of several practices involves the installation of in-stream structures that can mimic the effects of beaver dams (Nash et al., 2021; Pilliod et al., 2018; Wohl, 2021), often called beaver dam analogues (BDAs).

BDAs are becoming widely used by land managers across the western US to restore damaged streams, as well as to re-establish beaver populations. BDAs can be constructed by different methods. In some cases, they are built by piling logs on top of one another perpendicular to the channel (Wohl, 2021). As in this study, they can also be constructed by driving stakes across the stream, interweaving branches through the stakes, and then piling sediment on the upstream side of the structure. By pooling water, BDAs are presumed to reduce stream power and promote the aggradation of incised streams (Pollock et al., 2014). The modified water levels are also presumed to alter subsurface flow paths in the stream bed, the primary interest of this study.

One primary measure of stream bed flow paths is the vertical hydraulic gradient (VHG). VHG is a measure of water flux into or out of the stream via the stream bed. Vertical hydraulic gradients can be indicative of hyporheic exchange, as well as loss of stream water to groundwater or gain of groundwater into streams (Huang et al., 2016). Hyporheic exchange is characterized by bidirectional interaction between streamwater and shallow subsurface water (Bencala, 2005; Tonina & Buffington, 2009), which has been essential in downstream transport and in-stream processes, solute transfer, nutrient dynamics, and

biogeochemical cycling, and water temperature regulation (Bencala, 2005; Covino, 2017; Hester & Gooseff, 2010; Zarnetske et al., 2011).

Previous experimental and field studies have investigated several factors that can modify VHGs. In natural streams, shifts in the shape of the stream bed from convex to concave have been found to create regions of upwelling and downwelling (Anderson et al., 2005; Vaux, 1968). Relatedly, pool riffle sequences also create regions of upwelling and downwelling (Gooseff et al., 2006; Wondzell & Swanson, 1996), as do changes in bed slope, whether gradual (Harvey & Bencala, 1993) or rapid (Daniluk et al., 2013). Additionally, any debris or constructed barriers such as woody debris (Blaen et al., 2018; Wondzell et al., 2009), logs and log dams/ jams (Doughty et al., 2020; Fanelli & Lautz, 2008; Sawyer et al., 2011; Sawyer & Cardenas, 2012), beaver dams (Briggs et al., 2012, 2013; Jin et al., 2009; Lautz et al., 2006), and beaver dam analogues (Wade et al., 2020) can also generate vertical hydraulic gradients. In some situations, when the streambed slope is relatively flat, tight stream meander bends can induce lateral hyporheic exchange from water surface to water surface through the meander bend (Lautz et al., 2006; Wroblicky et al., 1998), leading to a higher gradient than would be expected from the channel slope alone.

An additional factor controlling VHG is the conductivity of the bed sediments (Hester & Doyle, 2008; Lewandowski et al., 2019). In studies evaluating the effects of stream structures, hydraulic conductivity has been established as an important factor controlling the magnitude of hyporheic exchange. Increases in hydraulic conductivity increase the downwelling flux rate and decrease hyporheic residence time (Hester & Doyle, 2008). These changes in flux due to adjacent but varying regions of bed permeability (i.e., adjacent high and low permeability regions) can induce changes in direction of VHG. Flow from a low permeability region into an adjacent high permeability region can create a downward VHG; conversely, flow from a high permeability region into a low permeability region can create an upward VHG (Vaux, 1968).

Aside from factors attributed to channel properties and processes, larger catchment characteristics also influence surface water-groundwater interactions. These include the size and spacing of channel units (Anderson et al., 2005); hillslope groundwater head under wet conditions (Harvey & Bencala, 1993); and the longitudinal gradient of the main valley floor relative to stream position (Wondzell & Swanson, 1996).

Despite numerous observations of variations in VHGs around channel structures, the vast majority of prior studies have primarily evaluated changes on only a limited number of structures over a relatively short section of channel reach (Table 1). Most of these studies have conducted monitoring on reaches of 100 m or less with a few that have been around 400 m. Furthermore, when stream structures are present, most studies have only evaluated flow dynamics around two or three structures. However, widespread stream restoration will likely only come from the widespread installation of structures. Indeed, natural systems have often been found to have beaver dam densities upwards of 10 in a kilometer (Briggs et al., 2012, 2013). Thus, there is a need to better understand the degree of spatial variation of VHGs when considered over long reaches with many structures.

The installation of 41 new BDAs and the upgrade of four existing BDAs along the entire Red Canyon Creek, Wyoming at the end of July 2021 provided a unique opportunity to observe the impacts of these structures on VHGs when present in a number far beyond previous studies. While prior studies have observed upwelling and downwelling patterns around individual stream structures in RCC (Lautz et al., 2006; Wade et al., 2020), there has been little assessment of such impacts over a long stream reach with multiple structures in sequence.

This study aims to identify changing patterns of VHGs before and after the installation of a large BDA complex and the controlling factors that determine these patterns. Three controlling factors are examined: (1) water depth above the stream bed, (2) interaction of the change in water surface elevation and distance, and (3) bed material. With the measurement of VHGs at varying distances from BDAs, the study can provide information on the spatial extent of the influence of BDAs on groundwater-surface water interactions. Ultimately, the observations will add to the growing knowledge of BDA impacts on surface water-groundwater interactions as well as inform how such restoration practices shape the overall hydrology, ecology, and biogeochemistry of semi-arid stream systems.

[Insert Table 1]

2. MATERIALS AND METHODS

2.1 Site Description

Our study site entails Red Canyon Creek (RCC) on The Nature Conservancy's Red Canyon Ranch site. RCC, a third-order stream, drains an 84-km² watershed near Lander, Wyoming (Figure 1A). RCC is fed by three major tributaries: Deep Creek, Barrett Creek, and Cherry Creek (Figure 1B) (Jin et al., 2010). The study site comprises a 1.2-km section of RCC approximately 0.5 km above its outlet to the Little Popo Agie River. The site consists of ranch lands sustainably managed by The Nature Conservancy (TNC). Flowing from south to north, with a channel slope of 0.3%-0.9% and average sinuosity of 2.3, RCC predominately receives summer baseflow from the slow release of groundwater that is recharged during spring snowmelt events (Davis et al., 2021; Lautz & Siegel, 2006; Pearce et al., 2021).

Prior work at this site and its tributaries, particularly Cherry Creek, has explored the effects of channel structures (Fanelli & Lautz, 2008; Lautz et al., 2006, 2010; Lautz & Fanelli, 2008), natural beaver dams (Briggs et al., 2013; Jin et al., 2009), and beaver dam analogues (Davis et al., 2021; Pearce et al., 2021; Wade et al., 2020) on stream function in RCC. The most recently installed structures at this site have been the BDAs. Prior to summer 2021, the site included four BDAs within the study reach, all installed between 2018 and 2020. In early August of 2021, these four BDAs were refurbished and construction of 41 new beaver dam analogues along the entire RCC was completed. A blown-out BDA, which was not refurbished, was also present along the reach. All in all, 45 functioning BDAs were present in RCC by mid-August 2021. Thirty-five of these (BDAs 12-46) fall within the 1.2-km reach that was examined in this study. The placement of the 35 BDAs in our study reach is shown in Figure 1C and Figure 1D. The remaining 10 were situated downstream of our study area. The BDAs were built from wood posts interwoven with willow and juniper and packed with sediment, mud, and streambed material. The streambed material was diverse, ranging from gravel and sand to clays. The structures were not built to the exact same dimensions, and water in the upstream pool varied in depth (Figure 5). However, all the BDAs were lower in the height than the surrounding banks (1.5 to 3 meters height in many cases as documented by Pearce et al. 2021), and none of the BDAs created pools that overflowed the channel banks into the flood plain.

Beyond the BDAs, it is useful to note other structures – natural and human – that were present in the study reach in 2021. Using the first installed mini-piezometer as a reference datum (Figure 1C), at approximately 325 m upstream, there was an intact log dam (Figure 2C) that was installed in the early 1990s (Lautz & Fanelli, 2008). Sediment has piled behind

this dam, but it did not appear to be backing up water during this observation period, such that there was no noticeable change in water elevation above or below this structure. At about 960 m upstream, a large, abandoned natural beaver dam was present (Figure 1D). This beaver dam actively backed up water, creating a pool approximately 1.5 meters deep that accumulated fine sediments and was included in this study (Figure 2B).

[Insert Figure 1]

[Insert Figure 2]

2.2 Field Data Collection

2.2.1 Measurement of VHGs

Vertical hydraulic gradients (VHG) were measured using mini-piezometers (Figure 3). The mini-piezometers were made from schedule 40, 1.22 cm (0.5 in) inner diameter PVC that had small holes drilled in the lower 10 cm of the pipe. Mini-piezometers were driven 30 cm into the stream bed using a slide hammer and installed from downstream to upstream. Unless limited by accessibility, the mini-piezometers were installed in the middle of the channel and spaced approximately 10 meters apart.

Mini-piezometers (n = 105) were first installed on July 16 and 17, 2021 prior to BDA installation; these were removed due to the construction of additional BDAs and refurbishment of the four within our study reach in late July and early August. A second set (n = 131) was installed from August 10 to 14, 2021 (post-BDA installation) (Figure 3A and Figure 3B). August mini-piezometers were installed at approximately the same location as the July installation, as determined using a GPS device, field notes, and photos.

In August 2021, we also installed several mini-piezometers at higher spatial densities at some locations to assess measurement precision and spatial variability:

- a. triplicates, spaced approximately 1 m apart as an equilateral triangle (Figure 3C), were installed at five locations to verify the repeatability of measurements; and
- b. triplicates, positioned across the channel as a transect, were installed above and below two consecutive BDAs (BDA 13 and BDA 14) (Figure 3D) and the natural beaver dam (Figure 3E) to assess lateral spatial variability in VHG across different types of stream structures.

During all experiments, mini-piezometers were left to equilibrate for at least 24 hours before measurements were completed. All mini-piezometers were measured on the same day within several hours. Specifically, measurements were done on July 18, 2021 during pre-BDA installation and August 17, 2021 during post-BDA installation. The August 17 date for post-BDA installation VHG measurement was intentionally selected such that the flow in the channel was similar to the flow in July. Details about the flow and stage during these dates are discussed in the Results section. Three measurements were made at each mini-piezometer: (1) depth to water inside the mini-piezometer; (2) depth to water outside the mini-piezometer; and (3) distance from the top of the mini-piezometer to the streambed.

Vertical hydraulic gradients (VHG) (m/m) were calculated following Anderson et al. (2005):

$$VHG = \frac{\Delta h}{\Delta l}$$
 Eqn. 1

where Δh is the elevation of water in the piezometer minus the elevation of the stream water surface, and Δl is the distance between the top of the screened interval to the surface of the stream bed. A positive VHG (i.e., flow from the bed toward the channel) represents upwelling, while downwelling occurs when the VHG is negative (i.e., flow from the channel into the bed).

[Insert Figure 3]

2.2.2 Analyses of controls on VHGs

We assessed three possible controls on spatial variability in VHG in the stream, both pre- and post-BDA installation: (a) influence of stream depth, (b) influence of interaction between the change in water surface elevation and distance, and (c) influence of streambed material characteristics. Univariate and multivariate linear regression analyses were performed to determine which explanatory variables control VHGs:

$$VHG = \beta_0 + \beta_1 X_1 + \cdots + \beta_n X_n + \varepsilon$$
 Eqn. 2

where X_l to X_n are vectors of the 1 to n explanatory variables, β_0 is the intercept, β_n are slope coefficients for each explanatory variable, and ε is the random error component. Initially, each explanatory variable was regressed with VHG alone. Additionally, to evaluate

the combined effects of all the variables on VHG, all potential controls were included a multivariate model. Residuals of regressions were assessed for any irregularities, but the residuals centered on zero and did not suggest strong non-linearities in the regression relationships, suggesting linear models were appropriate. Variables such as VHG and stream depth displayed some non-normality; we developed regressions with and without data transformations, but the outcome of the regressions changed little so we only present regression with non-transformed data. Model performance was evaluated using adjusted R^2 , p-value (presume significance at α =0.05), and Akaike Information Criterion (AIC). Data processing and statistical analyses were performed in R Statistical Software version 4.2.2 (R Core Team, 2022) using the dplyr package (Wickham et al., 2022) and the available functions in the base stats package (i.e., shapiro.test for normality test; wilcox.test for Mann-Whitney-Wilcoxon Test; kruskal.test for Kruskal-Wallis test; and Im for the linear regression).

Stream depth. Using the measurements associated with each mini-piezometer (discussed above), the stream depth was computed by subtracting the distance from the top of the mini-piezometer to the streambed by the depth to water outside the mini-piezometer.

Interaction between change in water surface elevation and distance. The influence of the interaction between the change in water surface elevation and distance was calculated differently before and after BDAs were installed. Prior to BDA installation in July 2021, this was taken as the water surface concavity calculated across successive mini-piezometers. Concavity (m/m^2) was calculated as the second derivative of water surface elevation (z) as a function of distance (x). The first derivative was calculated for non-uniform spacing between mini-piezometers using the equation of Anderson et al. (2005):

$$\frac{d}{dx}(z) = z(x_{i-1}) \frac{2x - x_i - x_{i+1}}{(x_{i-1} - x_i)(x_{i-1} - x_{i+1})} + z(x_i) \frac{(2x - x_{i-1} - x_{i+1})}{(x_i - x_{i-1})(x_i - x_{i+1})} + z(x_{i+1}) \frac{(2x - x_{i-1} - x_i)}{(x_{i+1} - x_{i-1})(x_{i+1} - x_i)}$$
Eqn. 3

where i indicates the relative spatial position and x and x_i were assumed to be the same minipiezometer. In computing for this, mini-piezometer 1, which is the most downstream location, was set as 0 m and cumulative distances were measured upstream from this location (Figure 4A). To calculate the concavity (i.e., second derivative), the results from the first derivative were plugged into the same equation. Note that while the form of the equation is

complex to account for unequal spacing between piezometers, it reduces to a basic centerdifferencing equation if intervals on the x-axis are presumed equal.

During post-BDA installation, concavity was no longer used because the BDAs led to level pool sections (Figure 5). Instead, the interaction between water surface elevation and distance was calculated as the hydrostatic pressure gradient across a BDA. The change in water elevation was determined by taking the difference between the water elevation upstream of the dam and the water elevation downstream of the dam. The gradient (m/m) was then computed by dividing the change in water surface elevation across the BDA by the distance of either the nearest upstream or downstream mini-piezometers around:

$$gradient = \frac{\Delta H}{\Delta L}$$
 Eqn. 4

where ΔH is equal to the water elevation difference across the BDAs and ΔL is the distance between the mini-piezometer and the nearest BDA. For mini-piezometers upstream of a dam, the initial elevation refers to the water elevation below the dam while the final elevation refers to the water elevation at the mini-piezometer above the dam. Conversely, for mini-piezometers downstream of a dam, the initial elevation refers to the water elevation at the top of the dam and the final elevation refers to the water elevation at the mini-piezometer below the dam (Figure 4B). The resulting gradients were therefore negative upstream and positive downstream.

[Insert Figure 4]

Streambed material characteristics. The assessment of stream bed material was primarily qualitative, using underwater images and in-field textural observations. The gross differences in the bed material collected around mini-piezometers were described by categorizing them as high gravel content and non-high gravel content. To validate if this system is appropriate, sediment samples were obtained around the immediate vicinity of a subset of the mini-piezometers (53 out of 105, and 20 out of 131 during pre- and post-BDA installation, respectively). Oven-dried samples of approximately 0.5 kg (dry weight) of bed material were passed through a set of sieves. Based on the unified system of classifying particle sizes

(Carter, 1993), particles with diameter greater than 2.00 mm are coarse sand to cobbles. In this study, these were grouped as gravel. A sample was considered high in gravel if the gravel component was >60% by weight, selected in part to maximize compatibility to the visual assessment. Of the 73 samples that were sieved, 67 samples had sieving data that agreed with the classification using visual analysis. This comparability between sieved samples and observations gave us high confidence that using the images and field notes alone is reasonably characterizing sediment type.

As described by Vaux (1968), transitions from higher permeability to lower permeability can result in upwelling. We, therefore, identified transitions from high permeability to low permeability between mini-piezometers (i.e., high gravel to non-high gravel content) starting from the most upstream installation location. At each transition where VHG increased by at least 0.056 (twice the value of the measured uncertainty associated with any VHG measurement as presented in Results) from either a negative or positive VHG, we determined whether the transition was from high to low permeability, based on our bed sediment classification. We then determined the statistical probability of an increase in VHG of at least 0.056 occurring randomly versus being associated with a change in sediment permeability. This consideration of sediment transition focused on the pre-BDA channel to avoid complicating factors from the sizable modifications to water elevations following the BDA installation; sediment deposits would not be expected to rapidly change so any influence of sediments on VHG was presumed to be most visible before BDA installation.

3. RESULTS

3.1 Stream profile and pattern of vertical hydraulic gradients

Prior to the installation of additional BDAs in July 2021, the study reach in RCC was largely characterized by shallow, high-velocity sections mixed with several deeper pools. The mean water depth at locations where mini-piezometers were installed was 0.27 m. An increase in stream water level was evident comparing post-BDA installation water levels (August 2021) with pre-installation water levels (July 2021). At points where mini-piezometers were installed, the mean depth increased to 0.51 m (Figure 5). Using a Mann-Whitney-Wilcoxon test, the stream depths along the study reach before and after BDA installation were found to be significantly different (W = 220, p-value = $< 2.2 \times 10^{-16}$).

The average discharge and accompanying stage at the point of flow measurement on the days of VHG measurement were 0.10 m³/s and 0.41 m in July and 0.12 m³/s and 0.45 m in August. Between these dates, the only sizeable rainfall that occurred was on July 30, 2021 (20.1 mm), which was 18 days before the post-BDA installation measurements. Thus, the vast majority of the increase in depths was attributed to the presence of the BDAs and not a change in flow. Changes in water elevation across the BDAs varied from 0.007 to 0.515 m.

[Insert Figure 5]

To evaluate the uncertainty in VHG measurements, differences among measurements in triplicate clusters were assessed. These measured difference in replicates was presumed to be indicative of the uncertainty in the VHG measurements. Each of the five clusters was broken into three pairs, providing 15 sets on which an average difference was calculated. The average difference across the 15 pairs was 0.028, indicating that the uncertainty associated with any VHG measurement was in the range of 0.028. Hence, the VHGs were categorized as upwelling for measurements greater than 0.028, downwelling for measurements less than - 0.028, and neutral for measurements between -0.028 to 0.028.

Also considered were variations in transects placed perpendicular to the stream axis used to assess lateral variability. Mini-piezometers in this configuration show an average paired difference in VHGs of 0.108, median of 0.075, and standard deviation of 0.130, in comparison to the average paired difference of 0.028, median of 0.026, and standard deviation of 0.022 for mini-piezometers in triangular configuration that were used to verify the repeatability of center-of-stream measurements. Two-sample Wilcoxon test indicates statistically significant differences between the median of the paired differences in VHG of these two configurations ($\alpha = 0.05$, W = 204, p-value = 0.012), suggesting that there may be additional lateral variability not accounted for in the way VHGs were measured in this study, given that mini-piezometers were installed at the center of the channel only. However, this lateral variation is still much less than the range in VHG seen longitudinally (-1 to 0.5) and is not presumed to obscure patterns seen from only looking at longitudinal variation, albeit the findings may be most reflective of conditions at the center of the channel.

In July 2021 prior to the 2021 BDA installation, the VHGs ranged from -1.16 to 0.29, with an average of -0.09. Around 11% (12 out of 105) of the mini-piezometers exhibited upwelling,

while 61% (64 out of 105) exhibited downwelling. The remaining 28% (29 out of 105) were within the neutral VHG range. Overall, these results indicate that the reach was a losing stream before the installation of the new BDAs.

After the installation of additional BDAs, VHGs ranged from -0.97 to 0.42, with an average of -0.12. The maximum downwelling and upwelling estimates were similar in magnitude to those observed pre-BDA installation. Downwelling remained the dominant vertical hydraulic gradient observed throughout the study reach, with 68% (89 out of 131) of the minipiezometers exhibiting downwelling. Only 14.5% (19 out of 131) showed upwelling while 17.5% (23 out of 131) showed VHGs within the neutral range. Changes in fraction of piezometers with upwelling before and after BDA installation were small and suggest minimal effect of the BDAs on upwelling behavior.

Based on a visual evaluation of the data, there was little correlation (Figure 6A) between VHG at similar locations before and after BDA installation, suggesting that non-BDA features do not strongly control VHG, as will be discussed in the following sections. As a further assessment, we considered the distribution of VHGs during both periods (Figure 6B). A Mann-Whitney-Wilcoxon test indicated that there was no statistical difference in the data distributions of VHGs pre- and post-BDA installation. To further rule out other possible spatial controls on VHG values, we constructed semivariograms, a measure correlation of measurements in space, with VHG observations, to investigate the potential for autocorrelation. The semivariograms approached the sill value at the smallest difference between points in this study, indicating no autocorrelative structure to the VHG data.

[Insert Figure 6]

High gravel material was the dominant bed sediment prior to BDA installation. Based on our qualitative assessment, 57% (60 out of 105) of mini-piezometer locations pre-BDA construction have streambed characterized by high gravel content. On the other hand, after the installation of additional BDAs in August, only 35% (46 out of 131) of mini-piezometer locations were clearly characterized by high gravel content. The bed sediment was also noticeably covered with a thin layer of silt during this period, which was presumed due to the disturbance caused by BDA construction. Along the study reach, there is no distinct pattern of sediments' influence on VHGs except at a few strong downwelling points behind dams,

which occurred in locations characterized by high fines content (Figure 7C). When considering pre-BDA installation, a Kruskal-Wallis test on the sediment data indicate that there is no significant difference on the median VHG among the different sediment types (Kruskal-Wallis chi-squared = 0.938, df = 1, p-value = 0.333). Post-BDA installation, a Kruskal-Wallis test identified significant difference in the median VHG among the different sediment types (Kruskal-Wallis chi-squared = 7.475, df = 1, p-value = 0.006).

[Insert Figure 7]

3.2 Controls on the vertical hydraulic gradient

Stream depth. Possible controls on VHG were considered pre- and post-BDA installation. The initial variable considered was water depth in the channel at each mini-piezometer. As mentioned above, post-BDA installation stream depths along the study reach were significantly different from pre-BDA installation depths (Figure 8A). In addition, there seemed to be a pattern that most downwelling occurred upstream of each dam (Figure 8B). However, there was no immediate visual evidence within the data that suggests water depth controls VHG, either before or after BDA installation. To quantitatively evaluate the possible role of different possible explanatory variables, a linear regression model between stream depth and VHGs was applied. For both pre-BDA and post-BDA installation, the univariate regression model (Table 2, Model 1) was not significant for $\alpha = 0.05$. For the pre-BDA installation, when stream depth was included with the other explanatory variables in the multivariate model (Table 2, Model 4), stream depth was the only significant variable. However, the model's adjusted R^2 is close to zero, indicating that the variable explains minimal variability in VHG during this period. During post-BDA installation, stream depth was not significant in the multivariate model.

[Insert Figure 8]

Interaction between change in water surface elevation and distance. The second variable that was considered for explaining VHG variation was the interaction of change in water elevation with distance along the stream axis. Pre-BDA installation, this was characterized as water surface concavity. When streambed characteristics are homogenous, VHGs are

expected to be negative for negative values of concavity and positive for positive values of concavity, with the magnitude increasing proportionally (Anderson et al., 2005). In RCC, concavity ranged from -6.63 x 10⁻⁴ to 6.52 x 10⁻⁴, with limited difference from reach to reach given the high sinuosity and low gradient along the reach. A visual comparison of concavity and VHG suggests that there is no evident relationship (Figure 9), and neither the univariate (Table 2, Model 2) nor multivariate linear regression (Table 2, Model 4) of concavity indicated that concavity was a statistically significant variable that can explain variations in VHG.

[Insert Figure 9]

For post-BDA observations, the role of water surface gradient (change in water elevation across the dam over distance from a dam) was assessed. A visual examination of gradient against VHG (Figure 10) shows greater downwelling and upwelling at points closest to a given BDA with downwelling above and upwelling below the BDA. Points farther from a dam do not exhibit significant upwelling or downwelling. Linear regression of VHGs against gradient show significant positive relationship between the variables. As apparent in Figure 10 and reinforced by the regression, as the gradient increases, the measured VHGs are also predicted to increase in magnitude (Table 2, Model 7).

When upstream and downstream gradients (relative to the BDA) are regressed separately with VHGs, upstream gradients show a larger adjusted R^2 (Table 2, Models 8 and 9), suggesting that the significant relationship between gradient and VHGs is stronger at locations above a dam. Both upstream and downstream gradients retained a significant relationship with VHG in a multivariate linear regression with other explanatory variables and the upstream gradient consistently had a higher coefficient than the downstream gradient (Table 2, Model 10). The difference in coefficient indicates that it is essential to treat the upstream and downstream gradient as separate explanatory variables.

[Insert Figure 10]

Streambed material characteristics. The final explanatory variable that was considered was the sediment characteristics. Sediment is not significant in the univariate model for pre-BDA installation (Table 2, Model 3). However, sediment is significant in both the univariate and

multivariate regression models for post-BDA installation (Table 2, Models 6 and 10, respectively), albeit only adding limited additional explanatory power given the small difference in adjusted R^2 between univariate gradient models and the multivariate model. The Kruskal-Wallis test does indicate that the median VHGs among the two sediment categories (i.e., high gravel vs non-high gravel) are significantly different, reinforcing the possibility that sediment characteristics have some –albeit – small contribution to VHG variations during post-BDA installation.

[Insert Table 2]

AIC was also used to assess model performance. For both BDA installation periods, the multivariate models (Table 2, Models 4 and 10) had the highest adjusted R^2 and lowest AIC. However, the multivariate model for pre-BDA installation VHG has a very low adjusted R^2 and does little to explain VHG during this period. In comparison, the adjusted R^2 of the multivariate model for post-BDA installation is at 0.694, with most of the variation explained by gradients created by the BDAs.

As an alternate analysis of the influence of streambed material on VHGs, the transitions in sediment characteristics along the study reach was assessed, considering that transition from high to low conductivity sediment can lead to upwelling. Examining the impact of sediment permeability pre-BDA (to eliminate the possibility of BDAs obscuring the role of sediments and at a period with less potential confounding variables), we found 24 transition zones from high to low permeability along our study reach (i.e., high gravel content to non-high gravel content). Among these transition zones, eight locations exhibited an increase in VHG that met or exceeded the 0.056 threshold in difference (i.e., twice the 0.028 average difference among triplicates) from the VHG measured in the previous mini-piezometer. The binomial distribution was used to assess if the transition in sediment permeability increased the likelihood of observing an increase in VHG between successive mini-piezometers. We evaluated whether the 8 out of 24 increases in VHG observed in the sediment permeability transition zones differed from the frequency of transition to increased VHG across all minipiezometers, which was observed in 36 out of 104 (34.6%) locations. The hypothesis test resulted in a p-value of 0.458 (greater than $\alpha = 0.05$) indicating that the probability of transitioning to an increased VHG occurring due to sediment permeability transition is not

significantly different from the random likelihood of observing a transition from lower to higher VHG.

4. DISCUSSION

Consistent with a prior study in Red Canyon Creek that only focused on three BDAs (Wade et al., 2020), the magnitude of VHG was found to mainly be dependent on the water level gradient established by the BDA, with downwelling above the BDA and upwelling or lower magnitude downwelling downstream of the BDA. However, expanding from such prior studies, mini-piezometer measurements in this study were extensive enough to also include points a sizable distance away from BDAs. The collection of numerous, spatially-distributed observations allowed for a more complete consideration of the net loss. Other studies of streambed exchange (e.g., Lautz et al., 2006; Storey et al., 2003) have noted gaining and losing sections, but measurements from these studies had focused only on short reaches of the stream, limiting inference over long reaches. Here, the approximately 100 repeated measurements at two different times provide a reasonably complete picture of distant spatial variations in stream water flux.

Despite several stretches of upwelling, the pre-BDA stream was consistently losing water (Figure 6A). With the addition of BDAs, strengthened upwelling and downwelling gradients were observed near BDAs. At more than several meters from BDAs, VHGs were consistently negative (downward), but with a slight net negative increase after BDA installation. This slight net negative increase in VHG suggests that the BDA complex may have a very minor mesoscale impact on surface water- groundwater interactions. This net negative increase is likely not detectable by studying only individual BDAs.

One factor that was not directly accounted for were changes in the water table height. It is possible that as the water table drops through the summer season, water table gradients also shift away from the stream. There were several wells in floodplain meadows adjacent to the BDA reach. These wells were approximately 5-10 meters from the stream. Water levels in these wells were closely related to the water level in the stream, increasing with the installation of BDAs. However, there were no wells farther away from the stream and no means to estimate changes in the water table gradient that may be driving subsurface water toward or away from the stream. Other studies evaluating controls on VHG (e.g. Anderson et

al., 2005; Wade et al., 2020) also were not able to quantify differences in the water table gradient.

There was an effort to use differential stream flow measurements to independently verify whether the stream was gaining or losing; separate flow measurements were taken at the upper and lower end of the BDA reach. However, there was no strong difference between the discharge above and below the BDA study reach, possibly due to the influence of irrigation diversions onto pastureland that adjoins the study reach. Despite this limitation, we are still able to estimate the quantity of water being lost through the stream bed and assess whether it is a physically plausible fraction of total streamflow (monthly average streamflow measured as 0.09 m³/s in July and 0.16 m³/s in August). Applying Darcy's Law, one can use the mean VHG (-0.09 in July 2021 prior to BDA installation and -0.12 in August 2021 after BDA installation), estimated hydraulic conductivity of the channel bed, and estimated channel bottom area. Hydraulic conductivity of 1 x 10 ⁻⁵ m s⁻¹ was estimated by multiple prior studies on the reach (Fanelli & Lautz, 2008; Lautz et al., 2010; Lautz & Siegel, 2006). Assuming a channel that is 1200 m long with channel width averaged from cross-sections at minipiezometers, the approximate area was calculated as 4930 m². Using these values, the estimated flux was 0.0047 m³ s⁻¹ and 0.0061 m³ s⁻¹ during pre- and post-BDA installation, respectively. These values are at 5% and 4% of the average discharge during July and August, respectively. Thus, the estimated loss is a physically reasonable fraction of the total flow.

While gradient was a moderately strong predictor of VHG in the post-BDA stream, not all variability in VGH could be explained in the post-BDA stream nor could variability be characterized in the pre-BDA stream. In part, one thing that cannot be readily explained is the change in the relationship between VHG and gradient upstream and downstream of a BDA, as evident in the difference in the coefficients in the regression model. This suggests that there are other factors affecting VHGs that are not easily characterized.

This challenge in explaining variations in VHG can in some part be attributed to the difficulty in measuring features, namely variations in sediment permeability (Anderson et al., 2005) and interaction with localized groundwater flow (Boano et al., 2014; Caruso et al., 2016). In terms of sediment, sediment samples were only collected 5 to 15 cm from the surface while the alluvial material underlying the stream is likely more than 1 m deep. Lautz et al. (2006)

characterized the subsurface as consisting of 2 m of alluvial sandy silt on top of 1 m of sand and gravel that rests on shale. In particular, areas identified in this study as having larger amounts of silt are most likely more quiescent zones with greater particle settling. However, there is a little indication there is parent material at depth that would have this same composition of low permeability particles.

Also complicating the explanation of VHGs are patterns in streamflow that can lead to subsurface flow paths that exit the stream channel (Boano et al., 2014; Payn et al., 2009). In particular, the presence of a meander may extend the distance over which water elevation changes when measured along the length of the channel, but water can also short circuit across the narrow neck of the meander (Wroblicky et al., 1998), creating a higher gradient that would be expected from channel measurements alone (Wondzell & Swanson, 1999). It is difficult to evaluate the role of meanders in generating flow short-circuiting without a formal groundwater model. However, we did selectively consider if tight meander bends were related to the highest magnitude VHG values as found in the pre-BDA stream (used to minimize additional variables). Of the six highest positive VHG values, none are near a meander. On the other hand, of the six most negative VHG values, three were associated with meanders: two were located near and above BDA 42 and the third one was located approximately 5m upstream of where BDA 35 was constructed (Figure 1D). Of these three, none exhibited the expected pattern of upwelling at locations after the meander, suggesting that presence of tight meanders in the stream did not influence the measured VHGs.

Also of consequence may be the choice of 10 meter spacing between mini-piezometers. While this 10-m spacing allowed quantification over more than 1 km of stream length, it limited quantification of the small-scale variations in gradients. Prior studies that have identified the role of concavity in hyporheic exchange have used 1 m intervals between piezometers (Anderson et al. 2005). Due to the physical labor required for piezometer installation, most studies will face limits to installing more than several hundred piezometers.

Finally, we note that these findings are specific to sampling scheme employed in Red Canyon Creek and, thus, may not be extended beyond this site. Measurements were limited to locations where mini-piezometers were installed, which are in the middle of the channel, and do not represent the lateral heterogeneity along the study reach. This limited spatial resolution may have missed to capture important BDA-induced changes and thus, contributes to the

uncertainties in the analysis. The analyzed controls on VHGs were also taken during baseflow and were shaped by weather conditions during summer 2021. Such conditions can vary from year to year and within season. Although ten supplemental measurements taken during May 2022 indicate similar patterns, these data still only represent short periods of time and do not necessarily represent the full range of conditions at the site or at BDAs.

5. CONCLUSIONS

This study aimed to identify patterns in vertical hydraulic gradients and their controlling factors during pre- and post-installation of beaver dam analogues on a mountain-recharge fed stream in the semi-arid west of the US. The majority of VHGs were negative, indicating that both pre- and post-BDA installation RCC is a losing stream. The distribution of VHGs during pre- and post-BDA installation were not found to be significantly different. Prior to BDA installation, there was no definitive explanatory variable that controlled spatial variation in VHG, with stream depth, stream surface concavity, and bed material having little influence. After BDA installation, the water level gradient across the BDA suitably explained much of the variation in VHG, with the strongest downwelling immediately upstream of a BDA and the strongest upwelling just downstream of a BDA. Of particular note, at more than a few meters from the BDAs, VHG was relatively small (near zero) and slightly negative during the mid-summer conditions.

This is one of the few studies of stream bed flux across a large BDA complex. Both before and after BDA installation, the stream was losing water to groundwater with only a slight increase in magnitude of loss after BDA installation. While BDAs did increase downwelling, this also resulted in higher upwelling such that the main influence of the BDAs appeared to occur within several meters of the BDAs. VHGs on portions of the stream more than several meters from the BDAs seemed little influenced by the presence of BDAs. At RCC, there is little evidence that the BDAs greatly changed the interconnections between surface water and groundwater, especially when more than several meters from a BDA.

These findings add to existing evidence that the size of a BDA's hydraulic step acts as a primary control on localized hyporheic exchange. When BDAs are intended to enhance hyporheic exchange, one may want to maximize the head drop across the BDA although it is

unclear what trade-offs in restoration goals may occur (i.e., higher head drop may lead to a less structural stability and more susceptibility to failure).

ACKNOWLEDGEMENTS

This work was funded with support from NSF Hydrologic Sciences Grant 15-558. The authors would also like to thank John Coffman of The Nature Conservancy in Wyoming, Eliza Hurst, Harold Jones, and Jeffrey Wade for providing their expertise and assistance during the fieldwork, and Charles Schirmer for his guidance and help in the processing of sediment samples.

DATA AVAILABILITY

The data that support the findings of this study are openly available in CUAHSI HydroShare at https://www.hydroshare.org/resource/9d25aa9097864c3ab69ac87099ab2c60/.

REFERENCES

- Anderson, J. K., Wondzell, S. M., Gooseff, M. N., & Haggerty, R. (2005). Patterns in stream longitudinal profiles and implications for hyporheic exchange flow at the H.J. Andrews Experimental Forest, Oregon, USA. *Hydrological Processes*, *19*(15), 2931–2949. https://doi.org/10.1002/hyp.5791
- Bakke, P. D., Hrachovec, M., & Lynch, K. D. (2020). Hyporheic process restoration: Design and performance of an engineered streambed. *Water*, *12*(2), 425. https://doi.org/10.3390/w12020425
- Bencala, K. E. (2005). Hyporheic Exchange Flows. *Encyclopedia of Hydrological Sciences*. https://doi.org/10.1002/0470848944.hsa126
- Blaen, P. J., Kurz, M. J., Drummond, J. D., Knapp, J. L. A., Mendoza-Lera, C., Schmadel, N. M., Klaar, M. J., Jäger, A., Folegot, S., Lee-Cullin, J., Ward, A. S., Zarnetske, J. P., Datry, T., Milner, A. M., Lewandowski, J., Hannah, D. M., & Krause, S. (2018).
 Woody debris is related to reach-scale hotspots of lowland stream ecosystem respiration under baseflow conditions. *Ecohydrology*, 11(5), 1–9.
 https://doi.org/10.1002/eco.1952

- Boano, F., Harvey, J. W., Marion, A., Packman, A. I., Revelli, R., Ridolfi, L., & Wörman, A. (2014). Hyporheic flow and transport processes: Mechanisms, models, and biogeochemical implications. *Reviews of Geophysics*, *52*, 603–679. https://doi.org/10.1002/2012RG000417
- Briggs, M. A., Lautz, L. K., & Hare, D. K. (2014). Residence time control on hot moments of net nitrate production and uptake in the hyporheic zone. *Hydrological Processes*, 28(11), 3741–3751. https://doi.org/10.1002/hyp.9921
- Briggs, M. A., Lautz, L. K., Hare, D. K., & González-Pinzón, R. (2013). Relating hyporheic fluxes, residence times, and redox-sensitive biogeochemical processes upstream of beaver dams. *Freshwater Science*, *32*(2), 622–641. https://doi.org/10.1899/12-110.1
- Briggs, M. A., Lautz, L. K., McKenzie, J. M., Gordon, R. P., & Hare, D. K. (2012). Using high-resolution distributed temperature sensing to quantify spatial and temporal variability in vertical hyporheic flux. *Water Resources Research*, 48(2), 1–16. https://doi.org/10.1029/2011WR011227
- Carter, M. (1993). Soil sampling and methods of analysis. Lewis Publishers.
- Caruso, A., Ridolfi, L., & Boano, F. (2016). Impact of watershed topography on hyporheic exchange. *Advances in Water Resources*, *94*, 400–411. https://doi.org/10.1016/j.advwatres.2016.06.005
- Covino, T. (2017). Hydrologic connectivity as a framework for understanding biogeochemical flux through watersheds and along fluvial networks. *Geomorphology*, 277(March), 133–144. https://doi.org/10.1016/j.geomorph.2016.09.030
- Daniluk, T. L., Lautz, L. K., Gordon, R. P., & Endreny, T. A. (2013). Surface water-groundwater interaction at restored streams and associated reference reaches. *Hydrological Processes*, 27(25), 3730–3746. https://doi.org/10.1002/hyp.9501
- Davis, J., Lautz, L., Kelleher, C., Vidon, P., Russoniello, C., & Pearce, C. (2021). Evaluating the geomorphic channel response to beaver dam analog installation using unoccupied aerial vehicles. *Earth Surface Processes and Landforms*, 46(12), 2349-2364. https://doi.org/10.1002/esp.5180
- Doughty, M., Sawyer, A. H., Wohl, E., & Singha, K. (2020). Mapping increases in hyporheic exchange from channel-spanning logjams. *Journal of Hydrology*, *587*, 124931. https://doi.org/10.1016/j.jhydrol.2020.124931
- Fanelli, R. M., & Lautz, L. K. (2008). Patterns of water, heat, and solute flux through streambeds around small dams. *Ground Water*, *46*(5), 671–687. https://doi.org/10.1111/j.1745-6584.2008.00461.x

- Gooseff, M. N., Anderson, J. K., Wondzell, S. M., LaNier, J., & Haggerty, R. (2006). A modelling study of hyporheic exchange pattern and the sequence, size, and spacing of stream bedforms in mountain stream networks, Oregon, USA. *Hydrological Processes*, 20, 2243–2457. https://doi.org/10.1002/hyp.6349
- Groß, J. (2003). Linear Regression. Springer-Verlag Berlin Heidelberg.
- Harvey, J. W., & Bencala, K. E. (1993). The effect of streambed topography on surface-subsurface water exchange in mountain catchments. *Water Resources Research*, 29(1), 89–98. https://doi.org/10.1029/92WR01960
- Hester, E. T., & Doyle, M. W. (2008). In-stream geomorphic structures as drivers of hyporheic exchange. *Water Resources Research*, *44*(3). https://doi.org/10.1029/2006WR005810
- Hester, E. T., & Gooseff, M. N. (2010). Moving beyond the banks: Hyporheic restoration is fundamental to restoring ecological services and functions of streams. *Environmental Science and Technology*, 44(5), 1521–1525. https://doi.org/10.1021/es902988n
- Huang, X., Andrews, C. B., Liu, J., Yao, Y., Liu, C., Tyler, S. W., Selker, J. S., & Zheng, C. (2016). Assimilation of temperature and hydraulic gradients for quantifying the spatial variability of streambed hydraulics. *Water Resources Research*, 52, 6419–6439. https://doi.org/10.1002/2015WR018408
- Hubbard, K. A., Lautz, L. K., Mitchell, M. J., Mayer, B., & Hotchkiss, E. R. (2010).
 Evaluating nitrate uptake in a Rocky Mountain stream using labelled 15N and ambient nitrate chemistry. *Hydrological Processes*, 24(23), 3322–3336.
 https://doi.org/10.1002/hyp.7764
- Janzen, K., & Westbrook, C. J. (2011). Hyporheic flows along a channelled peatland: Influence of beaver dams. *Canadian Water Resources Journal*, *36*(4), 331–347. https://doi.org/10.4296/cwrj3604846
- Jin, L., Siegel, D. I., Lautz, L. K., Mitchell, M. J., Dahms, D. E., & Mayer, B. (2010). Calcite precipitation driven by the common ion effect during groundwater-surface-water mixing: A potentially common process in streams with geologic settings containing gypsum. *Bulletin of the Geological Society of America*, 122(7–8), 1027–1038. https://doi.org/10.1130/B30011.1
- Jin, L., Siegel, D. I., Lautz, L. K., & Otz, M. H. (2009). Transient storage and downstream solute transport in nested stream reaches affected by beaver dams. *Hydrological Processes*, *23*(17), 2438–2449. https://doi.org/10.1002/hyp.7359

- Kasahara, T., & Hill, A. R. (2006). Effects of riffle-step restoration on hyporheic zone chemistry in N-rich lowland streams. *Canadian Journal of Fisheries and Aquatic Sciences*, 63(1), 120–133. https://doi.org/10.1139/f05-199
- Lautz, L. K., & Fanelli, R. M. (2008). Seasonal biogeochemical hotspots in the streambed around restoration structures. *Biogeochemistry*, *91*(1), 85–104. https://doi.org/10.1007/s10533-008-9235-2
- Lautz, L. K., Kranes, N. T., & Siegel, D. I. (2010). Heat tracing of heterogeneous hyporheic exchange adjacent to in-stream geomorphic features. *Hydrological Processes*, *24*(21), 3074–3086. https://doi.org/10.1002/hyp.7723
- Lautz, L. K., & Siegel, D. I. (2006). Modeling surface and ground water mixing in the hyporheic zone using MODFLOW and MT3D. *Advances in Water Resources*, *29*(11), 1618–1633. https://doi.org/10.1016/j.advwatres.2005.12.003
- Lautz, L. K., Siegel, D. I., & Bauer, R. L. (2006). Impact of debris dams on hyporheic interaction along a semi-arid stream. *Hydrological Processes*, *20*(1), 183–196. https://doi.org/10.1002/hyp.5910
- Lewandowski, J., Arnon, S., Banks, E., Batelaan, O., Betterle, A., Broecker, T., Coll, C., Drummond, J. D., Garcia, J. G., Galloway, J., Gomez-Velez, J., Grabowski, R. C., Herzog, S. P., Hinkelmann, R., Höhne, A., Hollender, J., Horn, M. A., Jaeger, A., Krause, S., ... Wu, L. (2019). Is the hyporheic zone relevant beyond the scientific community? *Water*, *11*(11). https://doi.org/10.3390/w11112230
- Nash, C. S., Grant, G. E., Charnley, S., Dunham, J.B., Gosnell, H., Hausner, M. B., Pilliod,
 D. S., & Taylor, J. D. (2021). Great Expectations: Deconstructing the Process
 Pathways Underlying Beaver-Related Restoration. *BioScience*, 71(3), 249–267.
 https://doi.org/10.1093/biosci/biaa165
- Payn, R. A., Gooseff, M. N., McGlynn, B. L., Bencala, K. E., & Wondzell, S. M. (2009). Channel water balance and exchange with subsurface flow along a mountain headwater stream in Montana, United States. *Water Resources Research*, 45(11). https://doi.org/10.1029/2008WR007644
- Pearce, C., Vidon, P., Lautz, L., Kelleher, C., & Davis, J. (2021). Impact of beaver dam analogues on hydrology in a semi-arid floodplain. *Hydrological Processes*, *35*(7). https://doi.org/10.1002/hyp.14275
- Pilliod, D. S., Rohde, A. T., Charnley, S., Davee, R. R., Dunham, J. B., Gosnell, H., Grant, G. E., Hausner, M. B., Huntington, J. L., & Nash, C. (2018). Survey of Beaver-related

- Restoration Practices in Rangeland Streams of the Western USA. *Environmental Management*, 61(1), 58–68. https://doi.org/10.1007/s00267-017-0957-6
- Pollock, M. M., Beechie, T. J., Wheaton, J. M., Jordan, C. E., Bouwes, N., Weber, N., & Volk, C. (2014). Using beaver dams to restore incised stream ecosystems. *BioScience*, 64(4), 279–290. https://doi.org/10.1093/biosci/biu036
- R Core Team. (2022). *R: A language and environment for statistical computing*. R Foundation for Statistical Computing. https://www.R-project.org/
- Sawyer, A. H., Bayani Cardenas, M., & Buttles, J. (2011). Hyporheic exchange due to channel-spanning logs. *Water Resources Research*, 47(8). https://doi.org/10.1029/2011WR010484
- Sawyer, A. H., & Cardenas, M. B. (2012). Effect of experimental wood addition on hyporheic exchange and thermal dynamics in a losing meadow stream. *Water Resources Research*, 48(10). https://doi.org/10.1029/2011WR011776
- Storey, R. G., Howard, K. W. F., & Williams, D. D. (2003). Factors controlling riffle-scale hyporheic exchange flows and their seasonal changes in a gaining stream: A three-dimensional groundwater flow model. *Water Resources Research*, *39*(2), 1–17. https://doi.org/10.1029/2002WR001367
- Tonina, D., & Buffington, J. M. (2009). Hyporheic exchange in mountain rivers I: Mechanics and environmental effects. *Geography Compass*, *3*(3), 1063–1086. https://doi.org/10.1111/j.1749-8198.2009.00226.x
- Vaux, W. G. (1968). Intragravel flow and interchange of water in a streambed. *Fishery Bulletin of the Fish and Wildlife Service*, 66(3), 479–489.
- Wade, J., Lautz, L., Kelleher, C., Vidon, P., Davis, J., Beltran, J., & Pearce, C. (2020).

 Beaver dam analogues drive heterogeneous groundwater–surface water interactions.

 Hydrological Processes, 34(26), 5340–5353. https://doi.org/10.1002/hyp.13947
- Welsh, M. K., Vidon, P. G., & McMillan, S. K. (2020). Stream and floodplain restoration impacts riparian zone hydrology of agricultural streams. *Environmental Monitoring and Assessment*, 192(2), 1–16. https://doi.org/10.1007/s10661-019-7795-3
- Wickham, H., Francois, R., Henry L., & Muller, K. (2022). *dplyr: A Grammar of Data Manipulation*. R package version 1.0.10. https://CRAN.R-project.org/package=dplyr
- Wohl, E. (2021). Legacy effects of loss of beavers in the continental United States. *Environmental Research Letters*, 16(2), 025010. https://doi.org/10.1088/1748-9326/abd34e

- Wondzell, S. M., LaNier, J., Haggerty, R., Woodsmith, R. D., & Edwards, R. T. (2009). Changes in hyporheic exchange flow following experimental wood removal in a small, low-gradient stream. *Water Resources Research*, 45(5), 1–13. https://doi.org/10.1029/2008WR007214
- Wondzell, S. M., & Swanson, F. J. (1996). Seasonal and storm dynamics of the hyporheic zone of a 4th-order mountain stream. I: Hydrologic processes. *Journal of the North American Benthological Society*, *15*(1), 3–19. https://doi.org/10.2307/1467429
- Wondzell, S. M., & Swanson, F. J. (1999). Floods, channel change, and the hyporheic zone. *Water Resources Research*, *35*(2), 555–567. https://doi.org/10.1029/1998WR900047
- Wroblicky, G. J., Campana, M. E., Valett, H. M., & Dahm, C. N. (1998). Seasonal variation in surface-subsurface water exchange and lateral hyporheic area of two stream-aquifer systems. *Water Resources*, *34*(3), 317–328. https://doi.org/10.1029/97WR03285
- Zarnetske, J. P., Haggerty, R., Wondzell, S. M., & Baker, M. A. (2011). Dynamics of nitrate production and removal as a function of residence time in the hyporheic zone. *Journal of Geophysical Research: Biogeosciences*, *116*(1), 1–12. https://doi.org/10.1029/2010JG001356

TABLES

Table 1. Studies on subsurface flow modification due to in-stream structures which used in-stream piezometers. The length of study reach was summed for those that were conducted in multiple reaches. The number of in-stream piezometers may also be the total number used or the maximum number installed if the study was conducted across different years.

Study	Site	Length of the study reach (m)	Type of in- stream structures present	Number of in-stream structures covered in the study	Number of in-stream piezometers used	Type of study	
Lautz and Siegel, (2006)	Red Canyon Creek, WY, USA	320	beaver dam, man-made (log) dam	5	11	physical hydrology	
Lautz et al. (2006)				3	5	physical hydrology	
(Hubbard et al., 2010)		~> 1000	debris dams, log dams, beaver dams	8	12	biogeochemistry	
Wade et al. (2020)		60	beaver dam analogues	3	47	physical hydrology and biogeochemistry	
Fanelli and Lautz (2008)	Red Canyon Creek and Cherry Creek, WY, USA	35	beaver dam, man-made (log) dam	3	54	biogeochemistry	
Lautz and Fanelli (2008)		15	man-made (log) dam	1	29	biogeochemistry	
Lautz et al. (2010)		~320	beaver dam, man-made (log) dam	2	6	physical hydrology	
Briggs et al. (2013)	Cherry Creek,	~25	beaver dams	2	9	biogeochemistry	
Briggs et al. (2014)	WY, USA	~25	beaver dams	2	9	biogeochemistry	
Kasahara and Hill (2006)	Silver Creek and Rouge River, Toronto, Ontario, Canada	~100	constructed riffles and steps	3	62, 52	physical hydrology and biogeochemistry	

Janzen and Westbrook (2011)	Bateman Creek, Sibbald Research Wetland, Canada	90	beaver dams	2	44	physical hydrology
Sawyer and Cardenas (2012)	San Antonio Creek, Valle Caldera National Preserve, New Mexico	175	logs	14	9	physical hydrology
Bakke et al. (2020)	Thorton Creek, Washington, USA	~110	engineered streambed enhancements	17, but only one was intensively studied	13	physical hydrology
Welsh et al. (2020)	Upper Yadkin Pee-Dee River Basin, North Carolina, USA	~85	cross vanes	2	40	physical hydrology

 Table 2. Regression analysis of factors controlling VHGs

Model	и	intercept	Stream depth	Concavity	Sediment (high gravel vs non-high	gradient	gradient (upstream)	gradient (downstream)	adjusted R ²	<i>p</i> -value	AIC
Pre-BDA installation											
1	105	-0.035	-0.220						0.018	0.090	-37.759
2	86	-0.062*		-2.101					-0.012	0.975	-81.710
3	105	-0.095*			-0.007				-0.009	0.811	-34.869
4	86	0.006	-0.269*	6.546	-0.002				0.038	0.106	-84.094
Post-B	DA insta	llation									
5	131	-0.017	-0.207*						0.025	0.038	-27.922
6	131	-0.108*			-0.075*				0.047	0.007	-30.915
7	131	-0.134*				2.069*			0.550	$< 2.2 \text{ x}$ 10^{-16}	- 129.146
8	62	-0.034					3.702*		0.682	$< 2.2 \text{ x}$ 10^{-16}	-60.036
9	69	-0.077*						0.860*	0.171	0.0002	- 121.032
10	131	-0.108*	0.103		-0.039*		3.451*	0.846*	0.694	< 2.2 x 10 ⁻¹⁶	- 176.546

^{*} significant at $\alpha = 0.05$

FIGURES

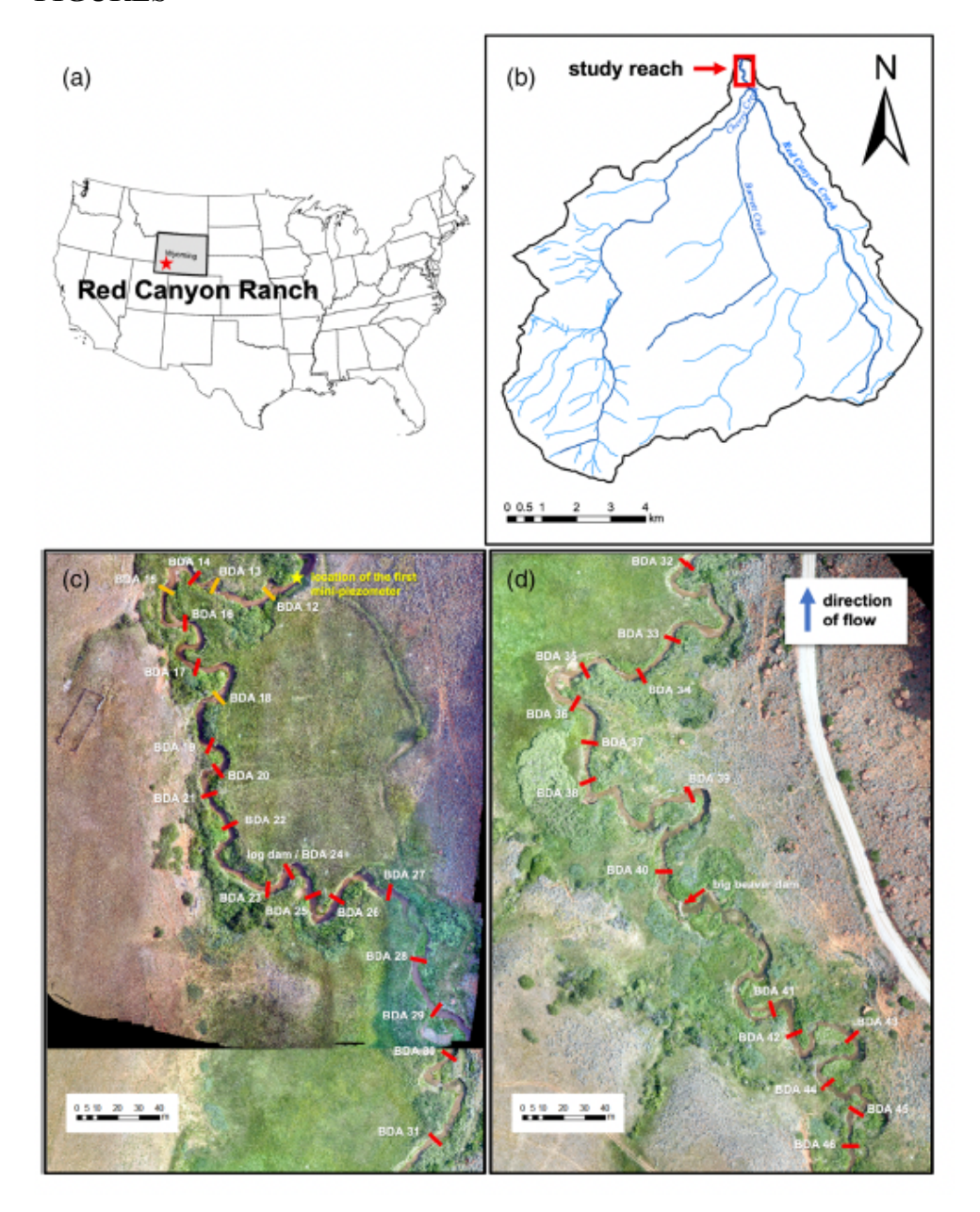


Figure 1. (A) Location of Red Canyon Ranch in the state of Wyoming; (B) location of the study reach at Red Canyon Creek, into which Barrett Creek and Cherry Creek drain; (C) lower reach, showing the location where the first mini-piezometer was installed, and the locations of BDAs 12-31; (D) upper reach, showing the locations of BDAs 32-46 and the location of the large beaver dam. BDAs 12, 13, 15, and 18 (in orange) are the BDAs that were present in the study reach in July 2021 prior to the installation of additional BDAs. The imagery was taken in July 2021 using an unmanned aerial vehicle (UAV). The black portions on the images are areas that were not covered by the UAV. Not visible in these images are the BDAs 1-11, which are not considered in this study.



Figure 2. Structures present on the studied reach in Red Canyon Creek prior to installation of additional beaver dam analogues: (A) BDA 13; (B) the large natural beaver dam (photo taken from the upstream side); and (C) log dam (photo taken from the upstream side).



Figure 3. (A) Installed mini-piezometer in July 2021; (B) installed mini-piezometer in August 2021. A and B are both mini-piezometer no. 29, which are approximately at the same location for both installation periods. (C) Mini-piezometers in clusters to verify the repeatability of measurements; (D) cluster of mini-piezometers above and below a BDA; and (E) cluster of mini-piezometers above the big natural beaver dam.

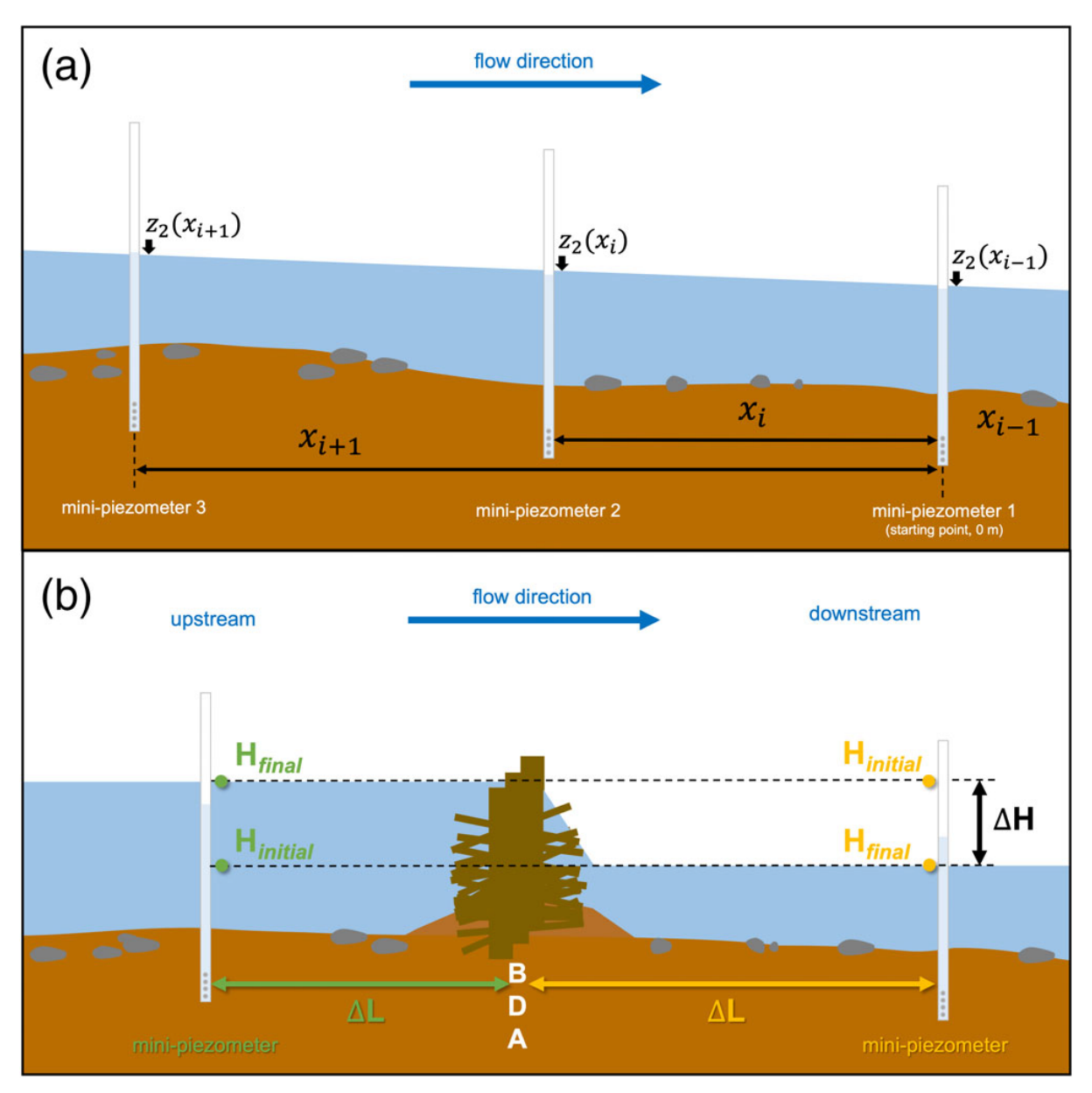


Figure 4. Schematic indicating dimensions used to compute (A) concavity pre-BDA installation (B) and gradient post-BDA installation.

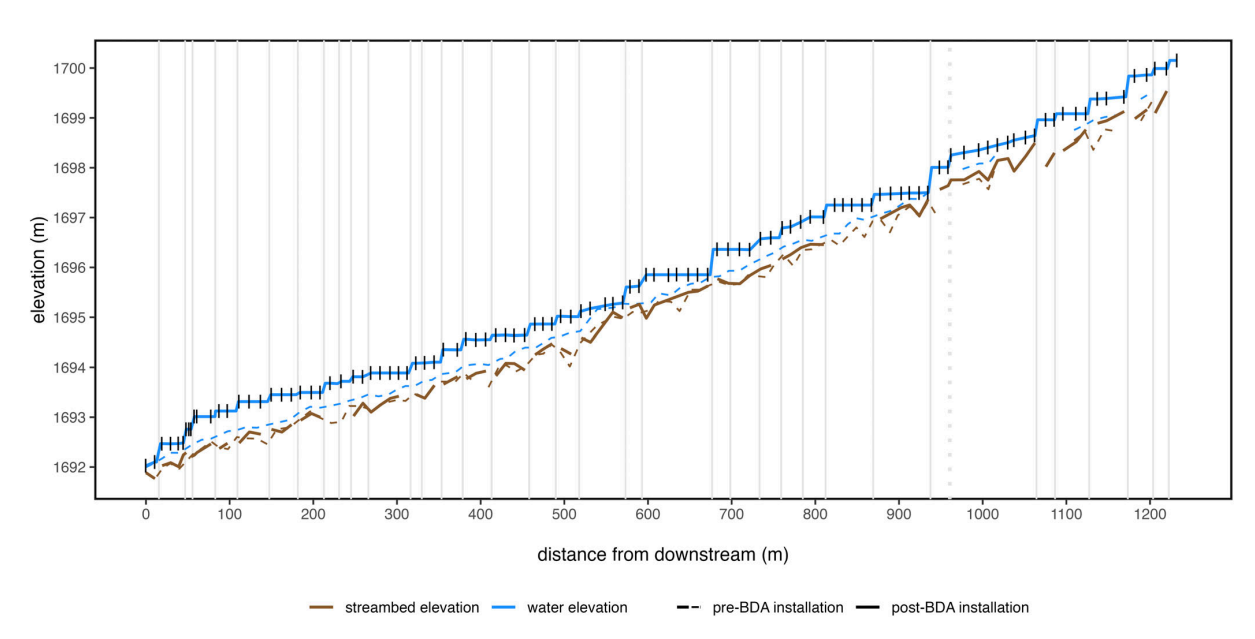


Figure 5. Stream profile of Red Canyon Creek before and after installation of BDAs. The solid gray vertical lines represent the BDAs and the dotted gray vertical line represents the large natural beaver dam present in the study reach. The small black vertical lines along the water elevation indicate the locations of the mini-piezometers post-BDA installation. An increase in the water level and a characteristic pattern of change in water elevation above and below a BDA are evident post-installation.

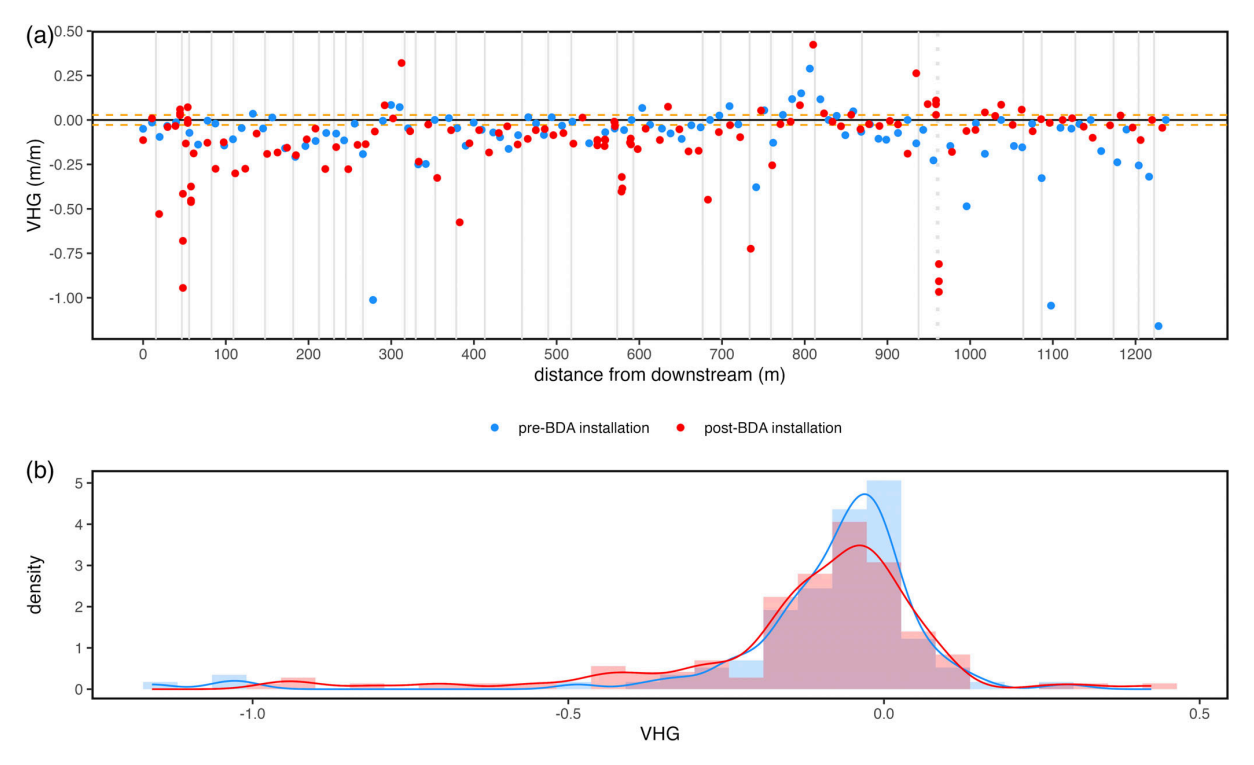


Figure 6. (A) Vertical hydraulic gradients at each mini-piezometer as measured pre- and post-BDA installation. The downstream datum (0 meters) is the most downstream mini-piezometer (installed approximately 15 meters downstream of BDA 12). The solid gray vertical lines represent the BDAs and the dotted gray vertical line represents the large natural beaver dam present in the study reach. The orange horizontal dashed lines represent the -0.028 to 0.028 range of measurement uncertainty. (B) Distribution of VHGs pre- and post-BDA installation.

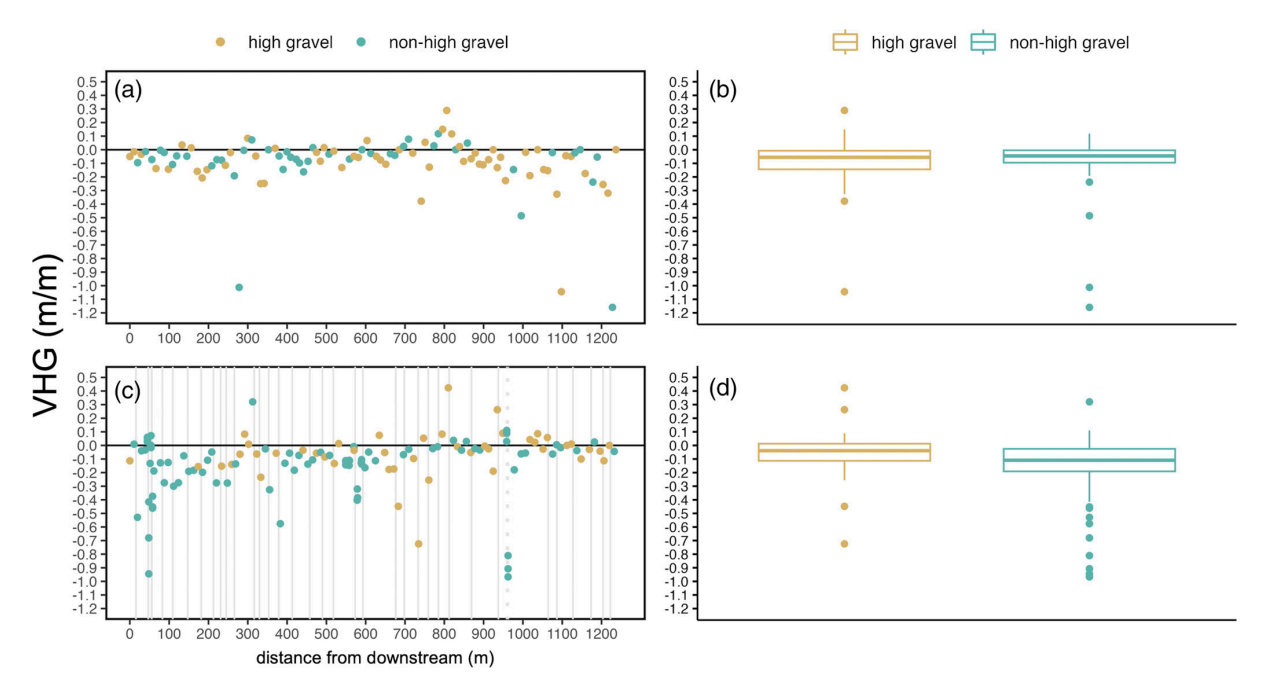


Figure 7. (A) Sediment characteristics in relation to VHG longitudinally along the study reach and (B) distribution of VHG relative to sediment classification pre-BDA installation; (C) and (D) are similar to (A) and (B) but for post-BDA installation.

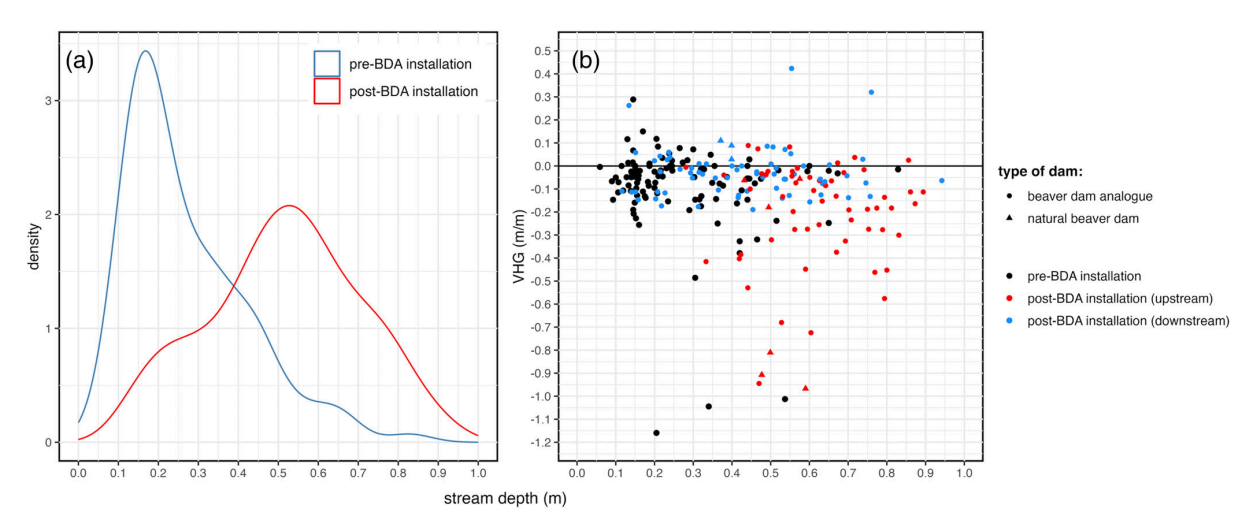


Figure 8. (A) Distribution of stream depth along the study reach pre- and post-BDA installation; (B) Influence of stream depth on the vertical hydraulic gradients measured pre- and post-BDA installation. Points for post-BDA installation are color-coded according to their location with respect to a beaver dam analogue or natural beaver dam: upstream = above the dam, downstream = below the dam. Points for post-BDA installation are also symbolized according to the type of dam they are closer to: beaver dam analogue or natural beaver dam.

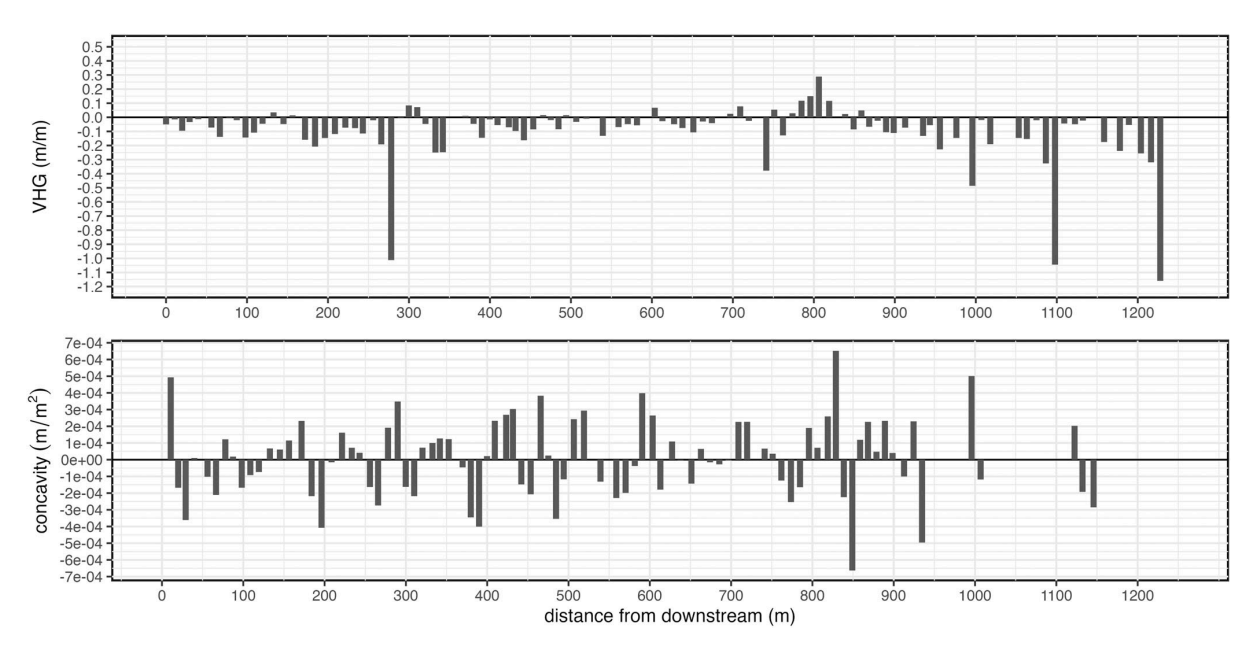


Figure 9. Measured vertical hydraulic gradients and concavity pre-BDA installation.

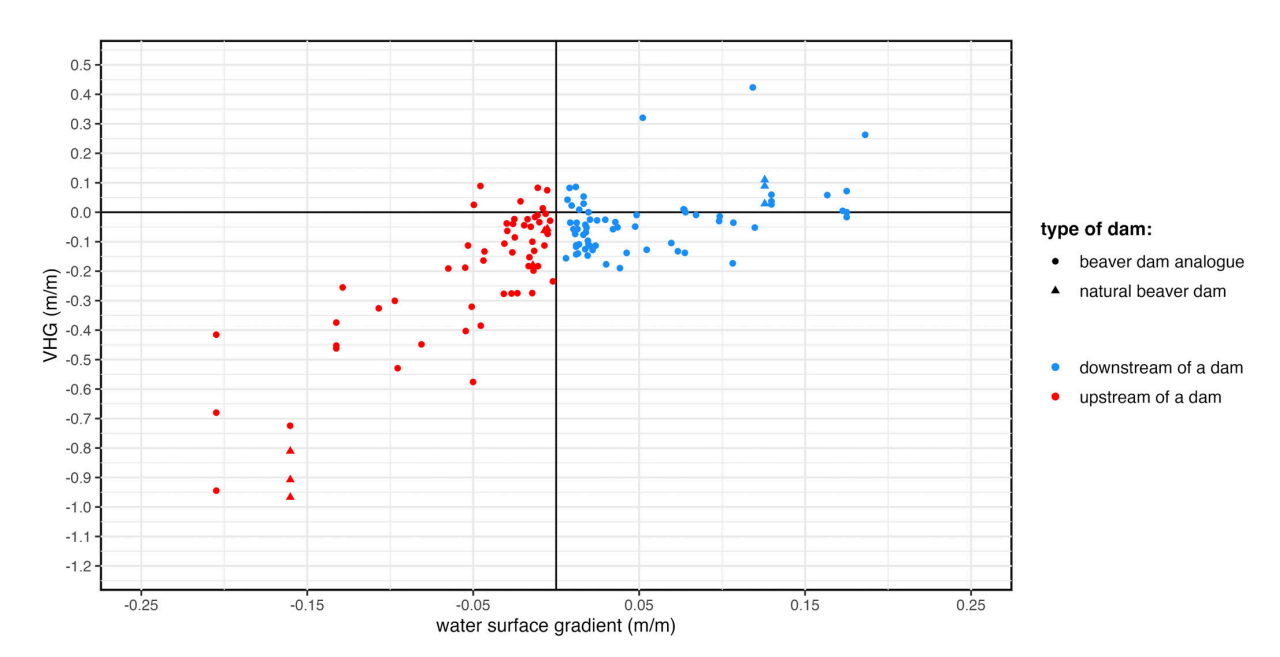


Figure 10. Influence of gradient (change in water elevation across the dam over distance to or from a BDA) to the VHGs measured post-BDA installation. Symbols represent the type of dam in close proximity to the sample point (i.e., beaver dam analogue or natural beaver dam) while the colors represent their location with respect to a dam (i.e., downstream or upstream).